Int. J. Appl. Math. Comput. Sci., 2003, Vol. 13, No. 3, 369–383

APPLICATION OF THE ADAPTIVE CENTER–WEIGHTED VECTOR MEDIAN FRAMEWORK FOR THE ENHANCEMENT OF cDNA MICROARRAY IMAGES

RASTISLAV LUKAC*, BOGDAN SMOŁKA**

* Slovak Image Processing Center
Jarkova 343, 049 25 Dobsina, Slovak Republic
e-mail: lukacr@ieee.org

** Institute of Automatic Control, Silesian University of Technology
ul. Akademicka 16, 44–101 Gliwice, Poland
e-mail: bsmolka@ia.polsl.gliwice.pl

In this paper a novel method of noise reduction in color images is presented. The new technique is capable of attenuating both impulsive and Gaussian noise, while preserving and even enhancing the sharpness of the image edges. Extensive simulations reveal that the new method outperforms significantly the standard techniques widely used in multivariate signal processing. In this work we apply the new noise reduction method for the enhancement of the images of the so called gene chips. We demonstrate that the new technique is capable of reducing the impulsive noise present in microarray images and that it facilitates efficient spot location and the estimation of the gene expression levels due to the smoothing effect and preservation of the spot edges. This paper contains a comparison of the new technique of impulsive noise reduction with the standard procedures used for the processing of vector valued images, as well as examples of the efficiency of the new algorithm when applied to typical microarray images.

Keywords: DNA microarray images, multichannel image processing, order-statistic theory, vector filters, impulsive noise

1. Introduction

Multichannel signal processing has been the subject of extensive research during the last decade, primarily due to its importance to color image processing. The most common image processing tasks are noise filtering and image enhancement. These tasks are an essential part of any image processing system, no matter whether or not the final image is utilized for visual interpretation or for automatic analysis (Mitra and Sicuranza, 2001; Pitas and Venetsanopoulos, 1990; Plataniotis and Venetsanopoulos, 2000).

It has been widely recognized that the processing of color image data as vector fields is desirable due to the correlation that exists among the image channels and to the fact that the nonlinear vector processing of color images is the most effective way to filter out noise. A number of nonlinear, multichannel filters which utilize the correlation among multivariate vectors using various distance measures were proposed (Astola and Kuosmanen, 1997; Mitra and Sicuranza, 2001; Pitas and Venetsanopoulos, 1990; Plataniotis and Venetsanopoulos, 2000). The most popular nonlinear, multichannel filters are based on the ordering of vectors in a predefined sliding window. The output of these filters is defined as the lowest ranked vector according to a specific ordering technique (Astola and Kuosmanen, 1997; Astola *et al.*, 1990). In this way, a set of reference vectorial filters, such as vector median filter (VMF) (Astola *et al.*, 1990), basic vector directional filter (BVDF) (Trahanias and Venetsanopoulos, 1993) and the directional distance filter (DDF) (Trahanias *et al.*, 1996), was developed. These nonlinear filters, based on the ordering operation, provide robust estimation in environments corrupted by bit errors, impulsive noise and outliers.

In general, the success of the searching for an image close to the undisturbed original depends on the complexity of the image scene, the nature of the corruption process and also on the accuracy of the adopted measures of the restoration (Astola and Kuosmanen, 1997; Bardos and Sangwine, 1997; Plataniotis and Venetsanopoulos, 2000).

Although the well-known vector filters hold good impulse noise attenuation characteristics, their performance is often accompanied with undesired processing of noise-free samples, which results in edge and texture blurring. The reason is that these nonlinear filters do not satisfy the superposition property (its nonlinearity is caused by the

ordering operation) and, thus, the optimal filtering situation can be never fully achieved.

In the case of the impulse noise corruption, the aim of the optimal filtering is to design noise reduction algorithms that would affect only corrupted samples, whereas the desired (noise-free) samples should be invariant under the filtering operation. This is realized by adaptive median filters, which replace the noisy samples by the median of the input set spanned by a filter window and perform the identity operation on the noise-free samples. The measure of the output distortion depends on the capability of the filters to detect atypical image samples—impulses and outliers, which can be very similar to samples belonging to an edge.

This paper focuses on a new nonlinear vector filtering scheme based on center-weighted vector median filters and robust order statistic theory to achieve optimal filtering properties. The proposed method improves the signal detail preservation capability and provides a higher flexibility of the filter design in comparison with the widely used VMF, BVDF and DDF techniques. In addition, its computational complexity is acceptable, which allows its application for the enhancement of DNA microarray images (Leung, 2002; Yang *et al.*, 2002). Using the new filtering scheme, it is possible to achieve an excellent balance between the signal-detail preservation and the noise attenuation. These properties of the proposed method were tested for a wide range of multichannel image signals, such as the standard color images (Lena and Peppers) and DNA artificial and real images.

The remainder of this paper is organized as follows. In the next section, the relevant vector filtering schemes such as VMF, BVDF, DDF and weighted vector median filters are described. In Section 3, we provide a new vector filter and analyze it in terms of detection operation, smoothing capability and signal-detail preservation. Section 4 is devoted to the analysis of the proposed methods depending on the intensity of impulsive noise corruption. This section also contains a number of simulations, tests and filtering results, together with tables and graphs depicting the objective image quality measures. We tested all relevant methods for standard color images and for DNA images, and also provided a short description of the microarray cDNA images. Finally, main ideas, results and suggestions for future work are summarized.

2. Multichannel Filtering Schemes

In multichannel image filtering, standard color images represent the vector-valued image signals, in which each image pixel can be considered as a vector of three components associated with the intensities of color channels consisting of red (R), green (G) and blue (B). Thus, it is necessary to consider the correlation that exists among the color channels and to apply the vector processing. If the existing correlation is not taken into account and color channels are processed independently, then the filtering operation is applied componentwise, (Fig. 1). In general, componentwise (marginal) approaches produce new vector samples, i.e., color artifacts, caused by the composition of reordered channel samples.

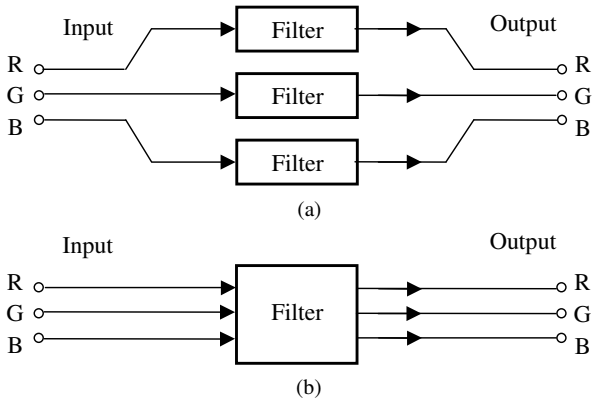

Fig. 1. Filtering methods for color images: (a) marginal filtering, (b) vector processing.

Vector filters represent a natural approach to the noise removal in multichannel images, since these filters utilize the correlation between color channels. For this reason, the vector methods represent the optimal and attractive approaches to denoising color images.

The most popular nonlinear, multichannel (vector) filters are based on the ordering of vectors in a predefined sliding window. The output of these filters is defined as the lowest ranked vector according to a specific ordering technique (Astola *et al.*, 1990; Peltonen *et al.*, 2001; Pitas and Tsakalides, 1991; Pitas and Venetsanopoulos, 1992; Smołka *et al.*, 2002; Tang *et al.*, 1995).

Let $y(x) : Z^l \rightarrow Z^m$ represent a multichannel image, where l is an image dimension and m characterises the number of channels. If $m \geq 2$, then it is the case of multichannel image processing. In the case of the standard color images, parameters l and m are equal to 2 and 3, respectively. Additionally, let $\mathbf{x}_1, \mathbf{x}_2, \ldots, \mathbf{x}_N$ be a set of input multichannel samples such that $\mathbf{x}_i \in Z^l$ for $i = 1, 2 \ldots, N$.

In general, the difference between two multichannel samples $\mathbf{x}_i = (x_{i1}, x_{i2}, \ldots, x_{im})$ and $\mathbf{x}_j = (x_{j1}, x_{j2}, \ldots, x_{jm})$ can be quantified through the commonly used Minkowski distance

$$\|\mathbf{x}_i - \mathbf{x}_j\|_\gamma = \left(\sum_{k=1}^{m} \left| x_i^k - x_i^k \right|^\gamma \right)^{\frac{1}{\gamma}}, \qquad (1)$$

where γ characterizes the employed norm, m is the dimension (number of channels) of vectors and x_i^k is the k-th element of the sample $\mathbf{x}_i$. Note that the well-known Euclidean distance corresponds to $\gamma = 2$.

Because vector filters respect the natural correlation that exists among color channels, each image sample is processed as a vector of channel intensities. The output of vector filters based on the robust order-statistic theory is defined as the lowest ranked vector, according to the specific ordering technique (Astola *et al.*, 1990; Bardos and Sangwine 1997; Gabbouj and Cheickh, 1996; Karakos and Trahanias, 1997; Lukac, 2001; Smołka *et al.*, 2002).

Let us consider an input sample $\mathbf{x}_i$, $i = 1, 2, \ldots, N$, associated with the distance measure L_i given by

$$L_i = \sum_{j=1}^{N} \|\mathbf{x}_i - \mathbf{x}_j\|_\gamma, \quad i = 1, 2, \ldots, N. \tag{2}$$

Another way to express the distance of multichannel samples is based on the angle between two multichannel samples $\mathbf{x}_i = (x_{i1}, x_{i2}, \ldots, x_{im})$ and $\mathbf{x}_j = (x_{j1}, x_{j2}, \ldots, x_{jm})$:

$$\mathrm{A}(\mathbf{x}_i, \mathbf{x}_j) = \cos^{-1}\left(\frac{\mathbf{x}_i \mathbf{x}_j^T}{|\mathbf{x}_i|\,|\mathbf{x}_j|}\right)$$

$$= \cos^{-1}\left(\frac{x_{i1}x_{j1} + x_{i2}x_{j2} + \cdots + x_{im}x_{jm}}{\sqrt{x_{i1}^2 + x_{i2}^2 + \ldots + x_{im}^2}\sqrt{x_{j1}^2 + x_{j2}^2 + \ldots + x_{jm}^2}}\right). \tag{3}$$

Let each input sample $\mathbf{x}_i$, for $i = 1, 2, \ldots, N$, be also associated with the sum of angular distances defined by

$$\alpha_i = \sum_{j=1}^{N} \mathrm{A}(\mathbf{x}_i, \mathbf{x}_j), \quad i = 1, 2, \ldots, N. \tag{4}$$

If the ordering criterion is expressed through products

$$\Omega_i = L_i \alpha_i, \quad i = 1, 2, \ldots, N, \tag{5}$$

$$\Omega_i = \sum_{j=1}^{N} \|\mathbf{x}_i - \mathbf{x}_j\|_\gamma \sum_{j=1}^{N} \mathrm{A}(\mathbf{x}_i, \mathbf{x}_j), \quad i = 1, 2, \ldots, N, \tag{6}$$

and the ordered set is given by

$$\Omega_{(1)} \le \Omega_{(2)} \le \cdots \le \Omega_{(N)}, \tag{7}$$

then the same ordering scheme applied to the input set results in the ordered sequence

$$\mathbf{x}^{(1)} \le \mathbf{x}^{(2)} \le \cdots \le \mathbf{x}^{(N)}. \tag{8}$$

The sample $\mathbf{x}^{(1)}$ associated with $\Omega_{(1)}$ represents the output of the directional distance filter (DDF) (Bardos and Sangwine, 1997; Trahanias and Venetsanopoulos, 1993; Trahanias *et al.*, 1996). Although the minimization of products $L_i\alpha_i$, $i = 1, 2, \ldots, N$ does not necessarily imply a minimum for either of L_i or α_i, it results in very small values for both of them. For that reason, the product minimization will select as a filter output the vector-valued sample that produces a very small sum of vector distances (2) and a very small sum of vector angles (4), simultaneously.

Let us assume the DDF with the power parameter p so that the power $1 - p$ is associated with the sum of vector distances and the power p (from interval $[0, 1]$) is associated with the sum of vector angles. Thus, Eqns. (5) and (6) can be simply rewritten respectively as

$$\Omega_i = L_i^{1-p} \alpha_i^p, \quad i = 1, 2, \ldots, N, \tag{9}$$

and

$$\Omega_i = \left(\sum_{j=1}^{N} \|\mathbf{x}_i - \mathbf{x}_j\|_\gamma\right)^{1-p} \left(\sum_{j=1}^{N} \mathrm{A}(\mathbf{x}_i, \mathbf{x}_j)\right)^p, \quad i = 1, 2, \ldots, N. \tag{10}$$

If $p = 0$, the DDF operates as the vector median filter (VMF) (Astola *et al.*, 1990), whereas for $p = 1$, the DDF is equivalent to the basic vector directional filter (BVDF) (Trahanias and Venetsanopoulos, 1993). For $p = 0.5$, the definition (9) is identical with (5), since the sum of vector distances and the sum of vector angles have equivalent importance.

Let $\mathbf{x}_1, \mathbf{x}_2, \ldots, \mathbf{x}_N$ be an input set determined by a filter window and N represent a window size. Let us assume that $w_1, w_2, \ldots, w_N$ represent a set of nonnegative integer weights so that each weight w_j, $j = 1, 2, \ldots, N$ is associated with the input sample $\mathbf{x}_j$. Then, it is possible to express the weighted vector distance J_i as

$$J_i = \sum_{j=1}^{N} w_j \|\mathbf{x}_i - \mathbf{x}_j\|_\gamma, \quad i = 1, 2, \ldots, N. \tag{11}$$

The sample $\mathbf{x}^{(1)} \in \{\mathbf{x}_1, \mathbf{x}_2, \ldots, \mathbf{x}_N\}$ associated with the minimal combined weighted distance $J_{(1)} \in \{J_1, J_2, \ldots, J_N\}$ is the sample that minimizes the sum of weighted vector distances. Note that the description

$$J_{(1)} \le J_{(2)} \le \cdots \le J_{(N)} \tag{12}$$

characterizes the ordered sequence of weighted vector distances. The sample $\mathbf{x}^{(1)}$ represents the output of the weighted vector median filter (WVMF) introduced in (Viero *et al.*, 1994). Equivalently, the WVMF can be defined by

$$\sum_{j=1}^{N} w_j \|\mathbf{y}_{WVMF} - \mathbf{x}_j\|_\gamma \le \sum_{j=1}^{N} w_j \|\mathbf{x}_i - \mathbf{x}_j\|_\gamma, \quad i = 1, 2, \ldots, N. \tag{13}$$

It is clear that in the dependence on the weight coefficients $w_1, w_2, \ldots, w_N$ the WVMF can perform a wide range of smoothing operations, so that the optimal weight vector can be found for each filtering problem.

3. Proposed Method

The vector median filter is designed to perform a "fixed" amount of smoothing. In many applications, it may become an undesired property and in some image applications the vector median filter introduces too much smoothing and blurs fine image details and even image edges. For that reason, the common problem is how to preserve some desired signal features when removing the noise elements with the vector median filter. An optimal situation would arise if a filter could be designed so that the desired features would be invariant to the filtering operation and only noise would be affected. Many contributions have provided different solutions to the problem of how to minimize the undesired effect of the vector median filtering using fuzzy logic, noise density estimations, subfilter structures and various restrictions imposed on the central sample (Lukac, 2002; 2003; Smołka *et al.*, 2001; 2002; Szczepanski *et al.*, 2002).

Ideally, the noise reduction filter should be designed in such a way that the noise-free samples should be invariant under the filtering operation and only noise-corrupted pixels should be affected by the filter action. In other words, in the case of noise-free samples, the filter should perform the identity operation (no filtering), whereas noisy samples should be replaced by the VMF. In order to provide an adaptive trade-off between the identity filter and the VMF, we present a new filtering scheme as a significantly simpler special case of the approaches introduced in (Smołka *et al.*, 2002), which makes use of various smoothing levels of the center-weighted vector median filters (CWVMFs).

Consider the weight vector given by

$$w_j = \begin{cases} N - 2k + 2 & \text{for } \ j = (N+1)/2, \\ 1 & \text{otherwise}, \end{cases} \tag{14}$$

i.e., the weight vector of nonnegative integer weights, where only the central weight $w_{(N+1)/2}$ associated with the central sample $\mathbf{x}_{(N+1)/2}$ can be changed, whereas other weights associated with the neighboring samples remain equal to one. Notice that $k = 1, 2, \ldots, (N+1)/2$ is a smoothing parameter. If the smoothing parameter k is equal to one, then the CWVMF is equivalent to the identity operation and no smoothing will be performed. In the case of $k = (N+1)/2$, the maximum amount of smoothing will be performed and the CWVMF filter is equivalent to the VMF. By varying k between 1 and $(N+1)/2$, it is possible to achieve the best balance between the noise suppression and the signal-detail preservation.

The CWVMF framework is more adequate for an adaptive filter design that will vary the smoothing levels in the filtering process, than the WVMF with a full set of weight coefficients (Alparone *et al.*, 1999; Viero *et al.*, 1994). Because of the complexity of the filter design related to the optimal setting of N weight coefficients, the WVMF optimization framework needs local or global optimization approaches to perform an optimal smoothing (Lucat *et al.*, 2002; Lukac *et al.*, 2003a; 2003b). Thus, the WVMF may fail in a situation with different statistical properties caused by an increased or a decreased noise probability or various distributions of the edges in the image. Note that the optimal WVMF filtering comes from optimization and filter design strategies used in gray-scale image filtering by means of weighted median (WM) filters, (a family of WM optimization approaches was summarized in (Yin *et al.*, 1996)).

The optimized WM filters are characterized by the same drawback (a fixed smoothing function) as the optimized WVMF filters. To remove this drawback, recent works (Chen and Wu, 2001; Chen *et al.*, 1999; Lukac and Marchevsky, 2001a) in the field of gray-scale image filtering provide adaptive methods based on the center-weighted median (CWM) filters or on equivalently defined lower-upper-middle (LUM) smoothers. The CWM (LUM) filtering structure is characterized by a tuning parameter, i.e., the center weight in CWM filters and the parameter for the smoothing in LUM smoothers. Let us denote this parameter by k. Varying the tuning parameter k, a class of CWM filters (LUM smoothers) allows the construction of a wide range of smoothing filters. Note that the adaptive designs use some kind of local control to choose the smoothing level which provides the best balance between the noise smoothing and signal-detail preservation.

The research of (Chen and Wu, 2001) brought the methodology of impulse detection based on the full set of CWM smoothing characteristics. Note that the CWM filter (LUM smoother) can be designed to perform $(N+1)/2$ smoothing realizations, including the identity operation and the well-known median filter. In this work, the detection operation is performed using the set of $(N+1)/2$ inequalities

$$\left\| \mathbf{y}_k - \mathbf{x}_{(N+1)/2} \right\|_\gamma \geq \mathrm{Tol}_k, \tag{15}$$

where $\mathbf{y}_k$ is the CWM output corresponding to the tuning parameter k, $x_{(N+1)/2}$ is a central (reference) sample of the sliding window and Tol_k is a fixed threshold. If any inequality defined by (15) is satisfied, the central sample is considered to be an impulse or an outlier. Note that for the increasing smoothing capability, (see Eqn. (14))

ranging from the identity filter (i.e., no smoothing corresponding to the maximum central weight) to the median filter (maximum smoothing for the central weight equal to one), the threshold values of adaptive CWM filters satisfy the condition

$$\mathrm{Tol}_1 \leq \mathrm{Tol}_2 \leq \cdots \leq \mathrm{Tol}_{(N+1)/2} \tag{16}$$

that corresponds to an increasing sequence

$$\begin{aligned}\left\|\mathbf{y}_1 - \mathbf{x}_{(N+1)/2}\right\| &\leq \left\|\mathbf{y}_2 - \mathbf{x}_{(N+1)/2}\right\| \\ &\leq \cdots \leq \left\|\mathbf{y}_{(N+1)/2} - \mathbf{x}_{(N+1)/2}\right\|. \end{aligned} \tag{17}$$

The presented approach with a 3×3 sliding window achieves very good results. However, because of the necessity of using all possible CWM filters, this way is very ineffective with the increasing window size. Thus it prohibits the straightforward optimization of necessary parameters and practically excludes the hardware implementation, especially for standard filtering with a 5×5 sliding window or in the field of image sequence filtering, where the spatiotemporal filters with a cube window of $N = 27$ samples are used, as the most practical approaches (Lukac and Marchevsky, 2001a; Viero *et al.*, 1994). Note that in this situation, the method of (Chen and Wu, 2001) would require $(N+1)/2 = 14$ CWM filters and the optimization of the same number of threshold parameters. The same extension would be also required in (Lukac and Marchevsky, 2001b), in which a similar approach to multichannel filtering was introduced. In order to decrease the number of smoothing levels and necessary thresholds, and to simultaneously simplify the optimization process, a new method working with a reduced set of smoothing levels was elaborated in (Lukac and Marchevsky, 2001a).

In order to avoid the above-mentioned drawbacks and make the filter design more flexible for changes in the basic filter parameters such as the size and the shape of the filter window, we provide the adaptive center weighted vector median filter (ACWVM) that will vary the extreme CWVM smoothing levels between the identity and the VMF operation. The proposed switching scheme is well suited for impulsive noise removal as it is able to filter only corrupted samples, whereas the desired image features are invariant to the filtering operation. The ACWVM is based on dividing the samples into two classes, namely probably corrupted samples and probably noise-free samples. As the decision tool for the central sample $\mathbf{x}_{(N+1)/2}$, the following rule is applied:

$$\begin{array}{llll} \text{IF} & \mathrm{Val} \geq \mathrm{Tol} & \text{THEN} & \mathbf{x}_{(N+1)/2} \text{ is impulse} \\ & & \text{ELSE} & \mathbf{x}_{(N+1)/2} \text{ is noise-free,} \end{array} \tag{18}$$

where 'Tol' is the threshold parameter and 'Val' is the aggregated sum of τ distances defined in (15),

$$\mathrm{Val} = \sum_{k=\lambda}^{\lambda+\tau} \left\|\mathbf{y}_k - \mathbf{x}_{(N+1)/2}\right\|_\gamma. \tag{19}$$

Here $\mathbf{x}_{(N+1)/2}$ is the central sample of the input set W, τ is a parameter (in this work we set $\tau = 2$), and $\mathbf{y}_k$ is the output of center-weighted median filter with the smoothing parameter k. If the parameter value Val is greater than or equal to the threshold value Tol, then the central input sample $\mathbf{x}_{(N+1)/2}$ is most probably corrupted and it will be processed by the VMF. In the case where the operation value Val is smaller than the threshold value Tol, the central sample $\mathbf{x}_{(N+1)/2}$ is most probably noise-free and it should be invariant to a filtering operation. Note that the proposed ACWVM filter requires only one threshold value in comparison with $(N+1)/2$ thresholds used in (Chen and Wu, 2001). In the case of color video filtering by spatiotemporal filters with a cube window, the proposed method will utilize the same number of 4 smoothing levels (three levels for the computation of the operation value Val and the maximum smoothing level for the impulse rejection), whereas in (Chen and Wu, 2001) 14 smoothing levels and the same number of thresholds have to be used.

4. Experimental Results

4.1. Experimental Results Achieved Using the Standard Color Images

In order to obtain the best performance of the proposed method, we performed some experiments related to setting parameters λ and Tol for a fixed value of $\tau = 2$. As the training images, we used the well-known test images (Figs. 2(a) and (b)) *Lena* and *Peppers* degraded by impulsive noise (Fig. 2(c)) (Astola and Kusmonen, 1997; Boncelet, 2000; Lukac, 2002; Lukac *et al.*, 2002; Plataniotis and Ventesanopoulos, 2000) given by

$$\mathbf{x}_{i,j} = \begin{cases} \mathbf{v} & \text{with probability } p_{\mathbf{v}}, \\ \mathbf{o}_{i,j} & \text{with probability } 1 - p_{\mathbf{v}}, \end{cases} \tag{20}$$

where i and j characterize the sample position, $\mathbf{o}_{i,j}$ is the original sample, $\mathbf{x}_{i,j}$ represents the sample from the noisy image, $p_{\mathbf{v}}$ is a corruption probability and $\mathbf{v} = (v_1, v_2, \ldots, v_m)$ is the noise vector of random intensity values.

From the results shown in Figs. 3 and 4 it can be observed that the optimal values of Tol and λ were found to be 80 and 2, respectively. Note that the achieved threshold value $\mathrm{Tol} = 80$ yields a sufficiently robust filter for a wide range of heavy-tailed noise characteristics and also

(a) (b) (c)

Fig. 2. Test images: (a) original image *Peppers*, (b) original image *Lena*, (c) *Lena* degraded by 10% impulsive noise ($p_{\mathrm{v}} = 0.1$).

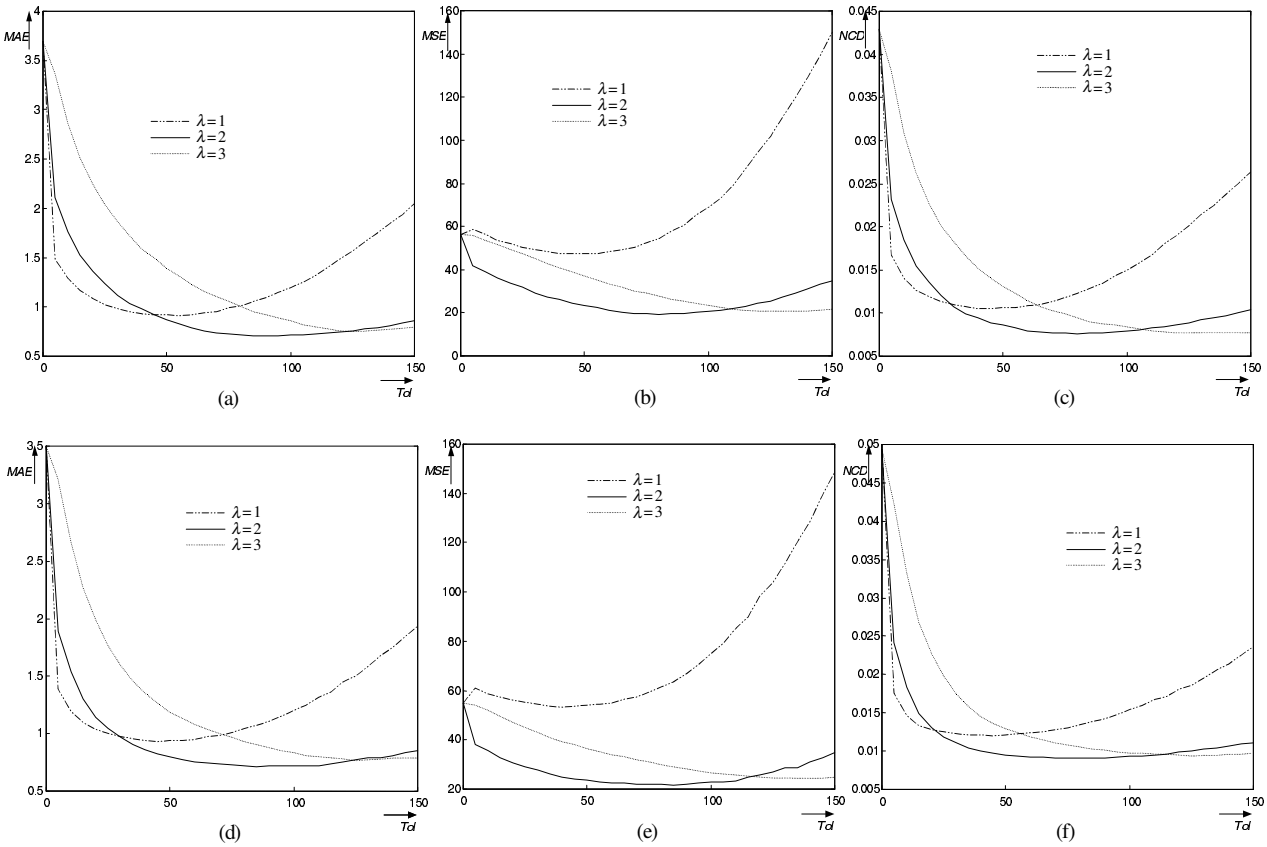

Fig. 3. Optimization of the proposed method for different parameters Tol and λ. The training set was given by the image *Lena*, cf. panels (a)–(c), and *Peppers*, cf. panels (d)–(f), with 10% impulsive noise.

for practical extensions of the 3×3 filter window to larger sizes and different shapes. Note that the proposed method includes the standard VMF filtering ($\mathrm{Tol} = 0$) and the identity operation ($\mathrm{Tol} \to \infty$) as special cases.

As regards the simplicity of the optimization process corresponding to the minimization of the chosen error criteria depending on the threshold value Tol, the proposed method can effectively adapt itself to changing noise and signal statistics, and therefore the optimal parameters $\mathrm{Tol} = 80$ and $\lambda = 2$ are sufficiently robust, as can be seen from the results depicted in Tabs. 1–5.

In general, the restoration quality of digital images is evaluated through the commonly used objective criteria (Plataniotis and Venetsanopoulos, 2000), such as the Mean Absolute Error (MAE), the Mean Square Error (MSE) and the Normalized Color Difference (NCD),

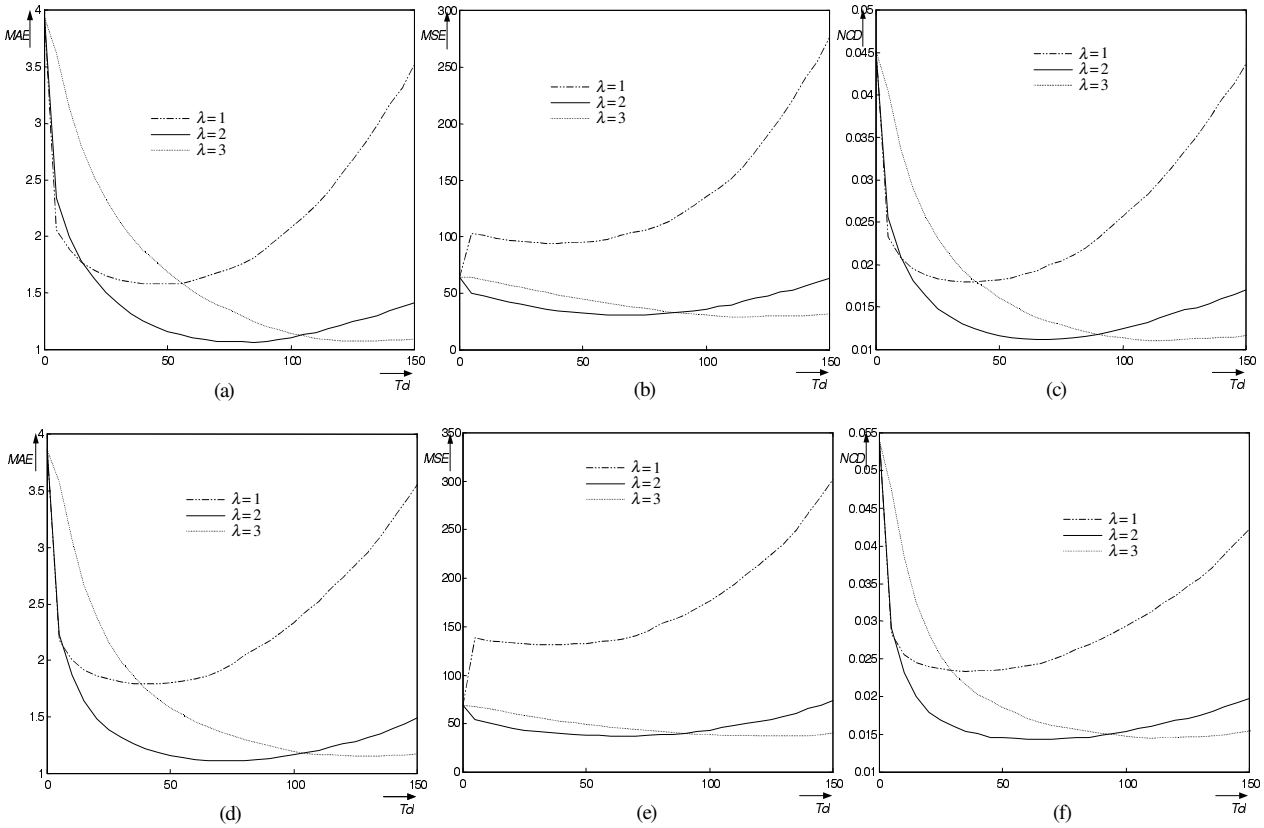

Fig. 4. Optimization of the proposed method for different parameters Tol and λ. The training set was given by the image *Lena*, cf. panels (a)–(c), and *Peppers*, cf. panels (d)–(f), with 15% impulsive noise.

which reflect the signal-detail preservation, the noise suppression and color chromaticity preservation. Mathematically, the MAE and the MSE are respectively given by

$$MAE = \frac{1}{NM}\sum_{i=1}^{N}\sum_{j=1}^{M}|o_{i,j} - x_{i,j}| \tag{21}$$

and

$$MSE = \frac{1}{NM}\sum_{i=1}^{N}\sum_{j=1}^{M}(o_{i,j} - x_{i,j})^2, \tag{22}$$

where $\{o_{i,j}\}$ is the original image pixel, $\{x_{i,j}\}$ is the filtered (restored) image pixel, i and j are indices of the sample position and N with M characterize the image size. In the case of color images, these criteria are computed as the means over color channels.

The NCD described in (Plataniotis *et al*, 1998; Plataniotis and Venetsanopoulos, 2000) expresses well the measure of the color distortion. The NCD is defined in the Lu*v* color space by

$$NCD = \frac{\frac{1}{NM}\sum_{i=1}^{N}\sum_{j=1}^{M}\sqrt{\left(L^{\mathbf{o}}_{i,j}-L^{\mathbf{x}}_{i,j}\right)^2+\left(u^{\mathbf{o}}_{i,j}-u^{\mathbf{x}}_{i,j}\right)^2+\left(v^{\mathbf{o}}_{i,j}-v^{\mathbf{x}}_{i,j}\right)^2}}{\frac{1}{NM}\sum_{i=1}^{N}\sum_{j=1}^{M}\sqrt{\left(L^{\mathbf{o}}_{i,j}\right)^2+\left(u^{\mathbf{o}}_{i,j}\right)^2+\left(v^{\mathbf{o}}_{i,j}\right)^2}}, \tag{23}$$

where $L^{\mathbf{o}}_{i,j}, u^{\mathbf{o}}_{i,j}, v^{\mathbf{o}}_{i,j}$ and $L^{\mathbf{x}}_{i,j}, u^{\mathbf{x}}_{i,j}, v^{\mathbf{x}}_{i,j}$ are values of the lightness and two chrominance components of the original image sample $\mathbf{o}_{i,j}$ and the noisy image sample $\mathbf{x}_{i,j}$, respectively.

It can be observed (Tables 1 and 2) that the proposed ACWVM filter (Fig. 5(f)) provides an improved signal-detail preservation capability in comparison with the standard vector filters such as the VMF (Fig. 5(c)), BVDF (Fig. 5(d)) and the WVMF (Fig. 5(e)). This kind of behavior is more visible in Fig. 6, which corresponds to the estimation errors of the above-mentioned methods. Note, that the WVDF is associated with the weight $[1,2,1,4,5,4,1,2,1]$ and the CWVMF with the smoothing parameter $k = 4$. The undesired effect of the blurring of fine image details introduced by the VMF, BVDF and DDF

Table 1. Results achieved using the test color image *Lena*.

Noise	5%			10%			15%		
Method	MAE	MSE	NCD	MAE	MSE	NCD	MAE	MSE	NCD
Noisy	3.762	427.3	0.0445	7.312	832.0	0.0840	10.707	1225.0	0.1230
VMF	3.430	50.8	0.0403	3.687	56.5	0.0429	3.939	64.5	0.0451
BVDF	3.818	58.6	0.0407	4.099	67.6	0.0432	4.405	81.4	0.0455
DDF	3.509	52.3	0.0402	3.733	57.3	0.0424	3.970	65.7	0.0444
WVMF	2.245	34.1	0.0265	2.537	43.6	0.0297	2.844	57.6	0.0324
CWVMF	1.740	25.0	0.0204	1.995	32.4	0.0232	2.264	43.3	0.0259
ACWVM	**0.417**	**12.0**	**0.0042**	**0.716**	**19.4**	**0.0076**	**1.067**	**31.5**	**0.0114**

Table 2. Results achieved using the test color image *Peppers*.

Noise	5%			10%			15%		
Method	MAE	MSE	NCD	MAE	MSE	NCD	MAE	MSE	NCD
Noisy	3.988	486.1	0.0441	7.677	943.3	0.0870	11.474	1402.4	0.1279
VMF	3.169	43.9	0.0452	3.503	55.0	0.0494	3.858	68.7	0.0541
BVDF	3.740	60.7	0.0438	4.151	82.7	0.0484	4.598	113.2	0.0532
DDF	3.182	44.6	0.0431	3.512	56.6	0.0475	3.844	70.8	0.0518
WVMF	1.835	25.0	0.0269	2.175	38.0	0.0316	2.615	58.6	0.0376
CWVMF	1.555	22.9	0.0219	1.836	32.5	0.0262	2.228	52.1	0.0316
ACWVM	**0.397**	**12.1**	**0.0045**	**0.724**	**21.9**	**0.0091**	**1.115**	**38.5**	**0.0146**

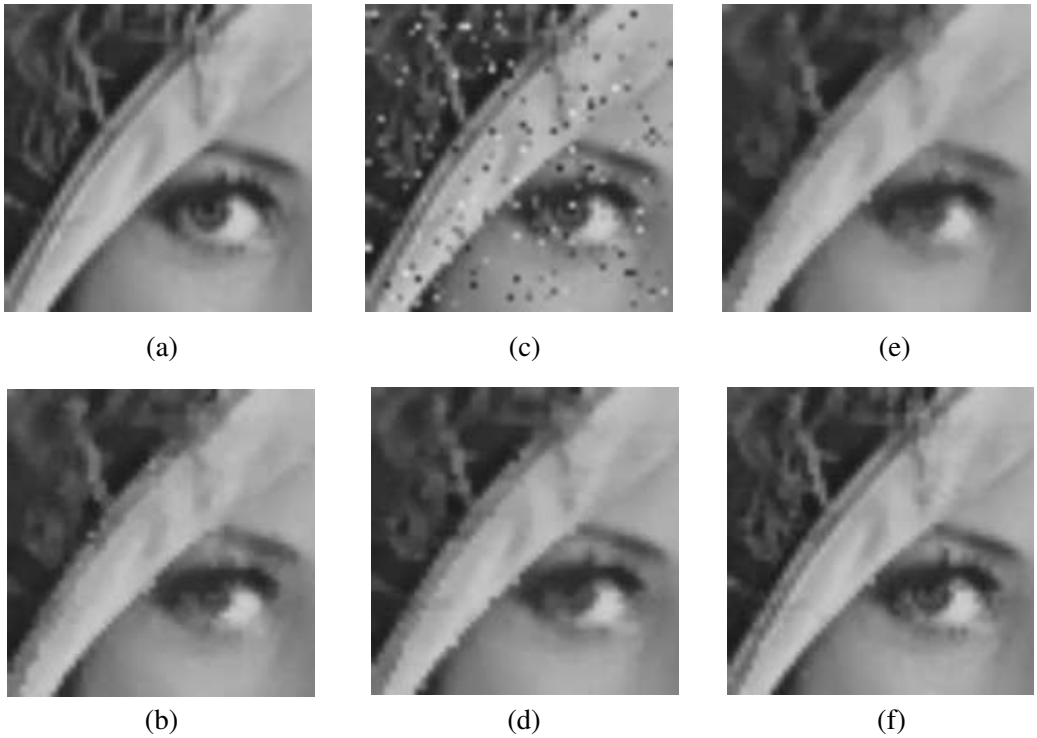

Fig. 5. Detailed view on the restored *Lena* image: (a) original image, (b) noisy image for $p_v = 0.1$, (c) VMF output, (d) BVDF output, (e) WVMF output with weights $[1, 2, 1, 4, 5, 4, 1, 2, 1]$, (f) output of the proposed method.

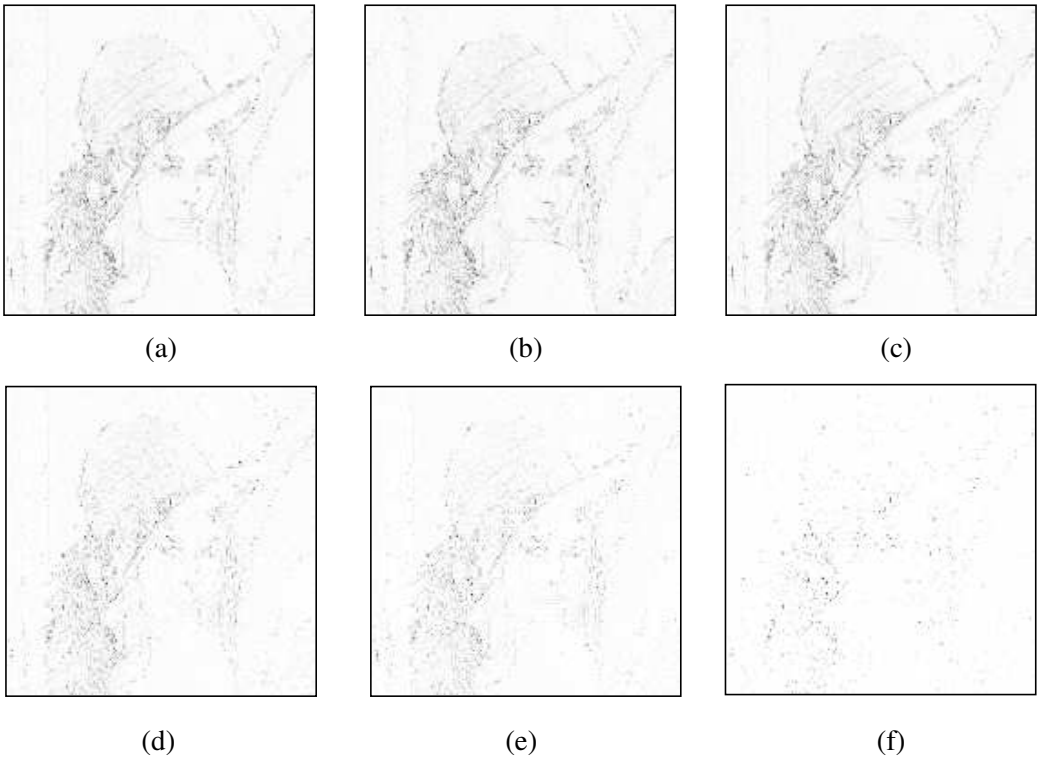

Fig. 6. Estimation errors of relevant filters using the image *Lena* degraded by impulsive noise with $p_v = 0.1$: (a) VMF, (b) BVDF, (c) DDF, (d) WVMF $[1, 2, 1, 4, 5, 4, 1, 2, 1]$, (e) CWVMF with $k = 4$, (f) proposed method—ACWVM.

is shown in Figs. 6(a)–(c). It can be easily observed that the standard filters suppress well impulses present in the image, yet some edges and image details are heavily blurred, especially at transitions between image regions. In the case of the BVDF, the increased estimation error (Fig. 6(b)) is caused by pure directional processing. In some situations, the decreased noise attenuation capability of the BVDF may result in the presence of impulses in the filtered image. Since the DDF combines the properties of both the VMF and BVDF, it suppresses noise well and reduces the edge jittering effect. The output of the proposed ACWVM filter, cf. Fig. 6(f), is characterized by an excellent balance between signal-detail preservation and noise suppression, which is reflected in the very small estimation error depicted in Fig. 6(f). The objective results evaluated by the commonly used measures such as MAE, MSE and NCD are listed in Tabs. 1 and 2. The proposed method excels significantly over all standard filtering schemes, and it also provides excellent balance between noise suppression and signal-detail preservation.

4.2. Experimental Results Achieved Using cDNA Images

The cDNA microarray is a popular and effective method for simultaneously assaying the expression of large numbers of genes (Chen *et al.*, 1997; Conway *et al.*, 2002; Dopazo, 2002; Eisen and Brown, 1999; Schena *et al*, 1995) and is perfectly suited for the comparison of gene expressions in different populations of cells.

A microarray is a collection of spots containing DNA, deposited on the surface of a glass slide. Each of the spots contains multiple copies of a single DNA sequence. In comparative gene expression experiments, the array is incubated with two cDNA probes, each of which is a mixture of cDNA's derived from the expressed mRNA of a distinct cell population. Each of the probes is labeled with a different fluorescent dye and then the labeled cDNA molecules hybridize to spots on the array containing their complementary sequences, the quantity of which is proportional to their concentrations. After hybridization, the amount of bound labeled cDNA on each spot is inferred from the intensity of fluorescence emitted when the spot is stimulated with a laser light.

The output of the assay at each spot is the ratio of cDNA concentrations in the two probes for each spotted sequence, as the fluorescent intensities are not calibrated to absolute amounts of DNA. Once the cDNA probes have been hybridized to the array and loose probes have been washed off, the array is scanned to determine how much of each probe is bound to each spot. The probes are tagged with fluorescent reporter molecules which emit detectable light when stimulated by the laser. The emitted light is

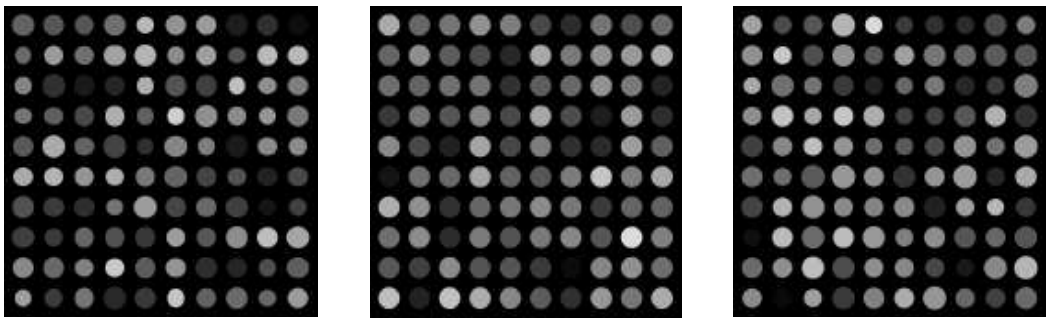

(a) (b) (c)

Fig. 7. Artificial cDNA microarray test images: (a) DNA1, (b) DNA2, (c) DNA3.

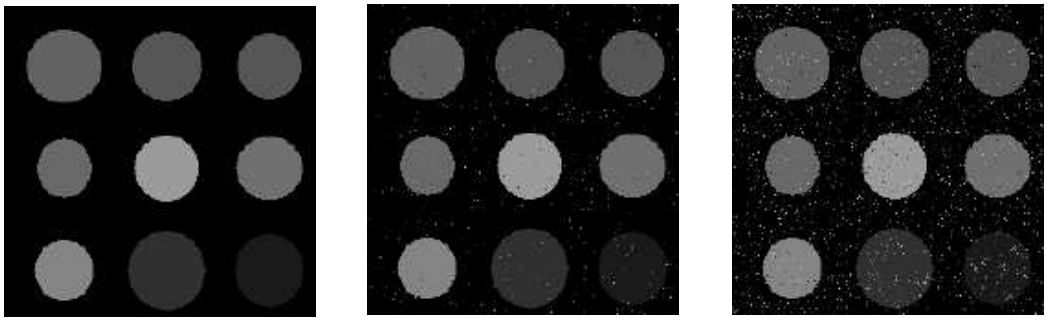

(a) (b) (c)

Fig. 8. Detailed view on test images: (a) original DNA1, (b) 1% impulsive noise, (c) 10% impulsive noise.

captured by a detector (a CCD or a confocal microscope) which records the light intensity. When the laser scans the entire slide, a large array image containing thousands of spots is produced. The spots occupy a small fraction of the image area and they have to be individually located and isolated from the image background prior to the estimation of its mean intensity. The fluorescent intensities for each of the two dyes are measured separately, producing a two-channel image. The image is false colored using red and green for each image component, which represents the light intensity emitted by the two fluorescent dyes. So the microarray images look like a collection of green, red and yellow spots of different hue, saturation and intensity. Spots whose mRNA's are present at a high level in one or the other cell population show up as predominantly red or green. The intensities provided by the array image can be quantified by measuring the average or integrated intensities of the spots. The ratio of the fluorescent intensities for a spot is interpreted as the ratio of concentrations for its corresponding mRNA in the two-cell populations.

The quantitative evaluation of microarray images is a difficult task. The major sources of uncertainty in spot finding and measuring the gene expression are variable spot sizes and positions, variations in the image background and various image artifacts. Spots vary significantly in size and position within their vignettes, despite the use of precise robotic tools to lay them out onto the slide. Additionally, the natural fluorescence of the glass slide and non-specifically bounded DNA or dye molecules add a substantial noise floor to the microarray image. To make the task even more challenging, the microarrays are also afflicted with discrete image artifacts such as highly fluorescent dust particles, unattached dye, salt deposits from evaporated solvents, fibers and various airborne debris (Ajay *et al.*, 2002; Bozinov and Rahnenführer, 2002; Filkov *et al.*, 2002; Hsiao *et al.*, 2002).

In order to compare the performances of the applied filtering schemes, we used a set of artificial images (Fig. 7), and also natural microarray images (Fig. 12). Using the artificial images, we can also evaluate the objective restoration criteria, because the original, undistorted images are available. In the case of the natural cDNA images, we can compare only the subjective results in the form of a visual assessment of the filter outputs.

To evaluate the achieved results, objective criteria such as the mean absolute error (MAE) and the mean square error (MSE), which reflect the signal-detail preservation and the noise suppression respectively, were used. As can be seen (Tables 3–5, Figs. 10 and 11) the proposed method outperforms significantly the commonly-used multichannel noise reduction techniques. This is also confirmed by its performance on real images, (Figs. 13–16), in which the noise component was successfully removed while preserving the sharpness of the spot edges.

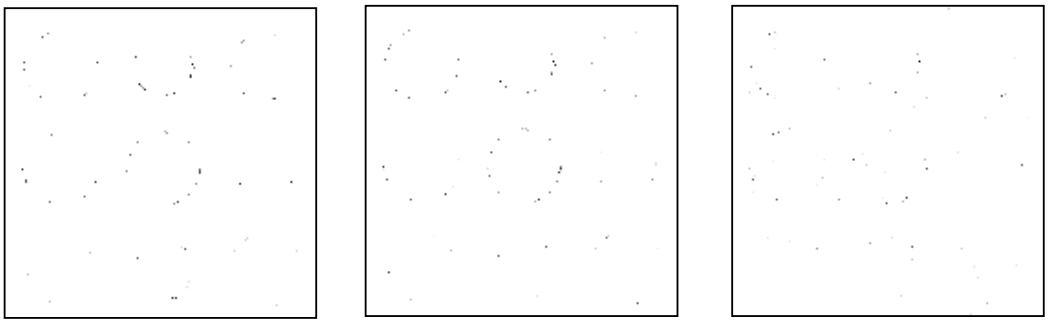

(a) (b) (c)

Fig. 9. Emphasized estimation errors of relevant filtering schemes applied to a 10% impulsive noise: (a) VMF, (b) BVDF, (c) ACWVM (proposed method).

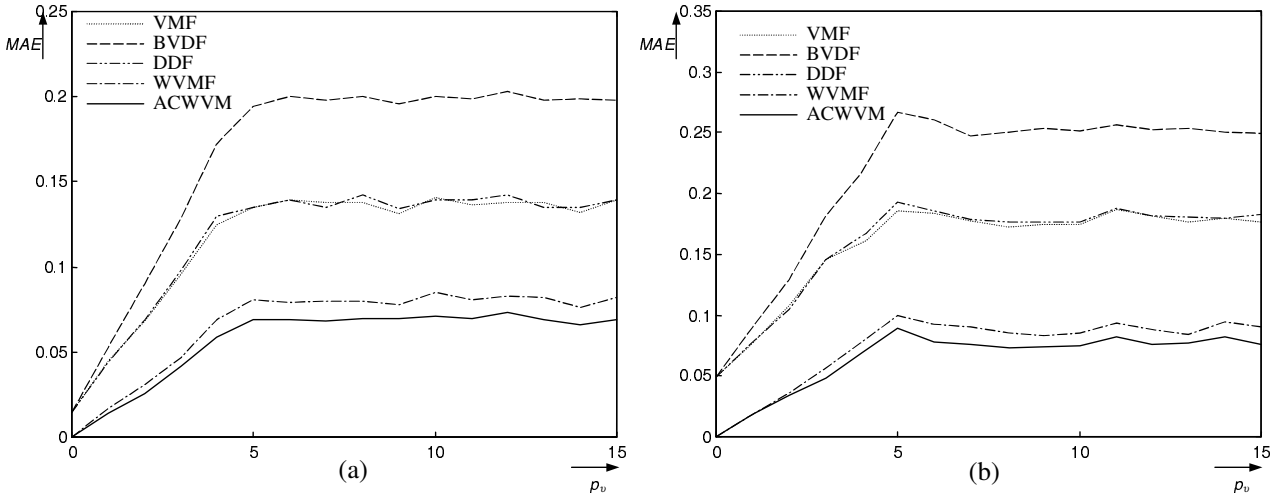

Fig. 10. Dependence of the MAE criteria on the impulsive noise probability: (a) test image DNA1, (b) test image DNA3.

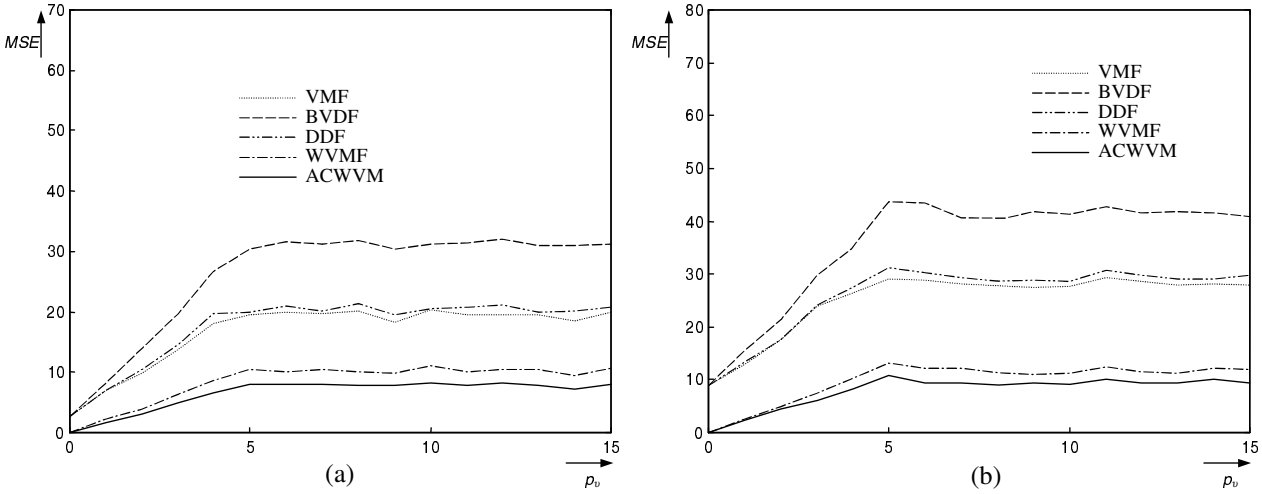

Fig. 11. Dependence of the MSE criteria on the impulsive noise probability: (a) test image DNA1, (b) test image DNA3.

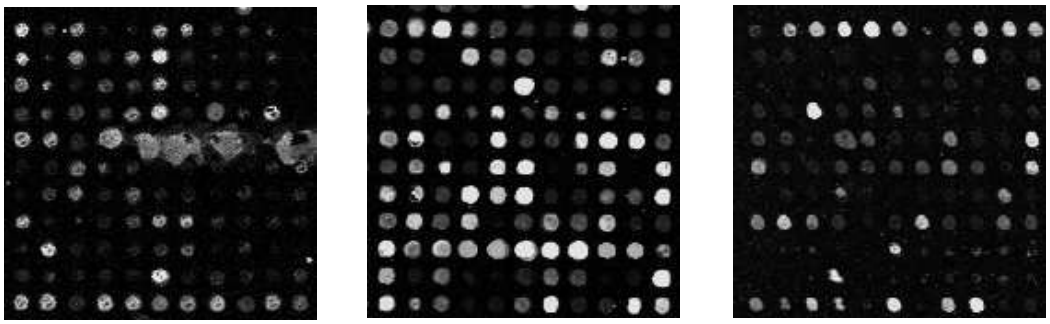

(a) (b) (c)

Fig. 12. Real cDNA test microarray images.

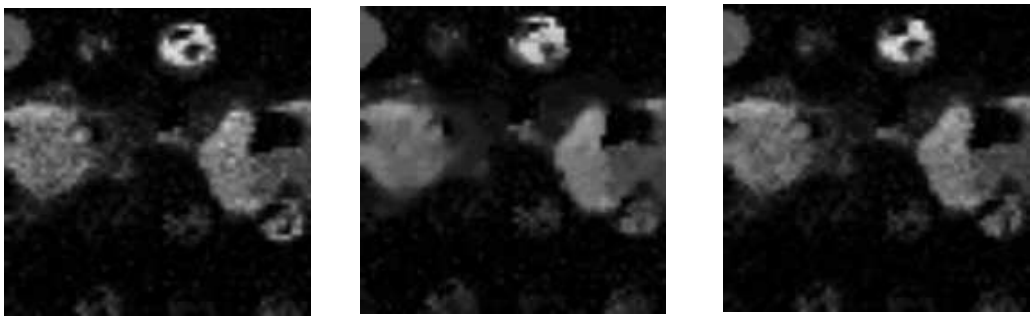

(a) (b) (c)

Fig. 13. Experimental results achieved using real DNA images: (a) observed image, (b) VMF output, (c) ACWVM output.

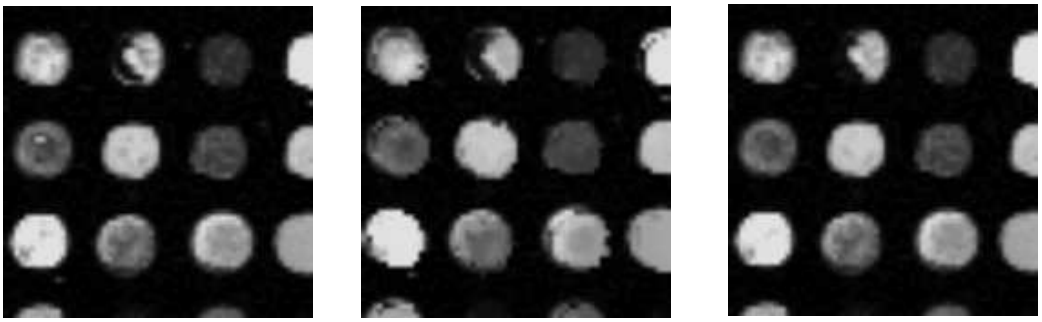

(a) (b) (c)

Fig. 14. Experimental results achieved using real cDNA images: (a) noisy image, (b) VMF output, (c) ACWVM output.

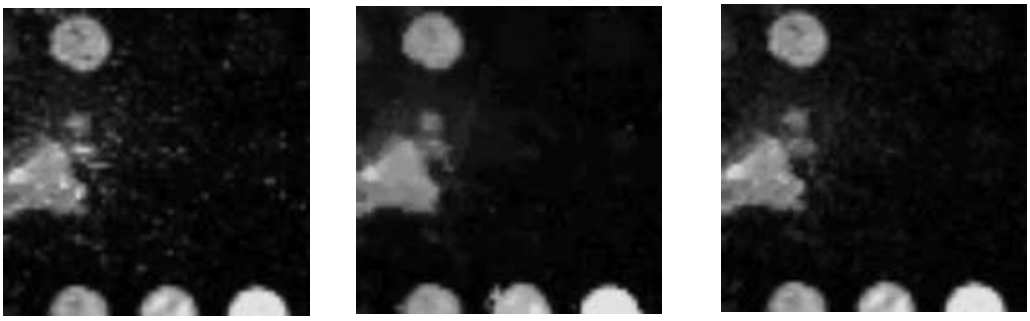

(a) (b) (c)

Fig. 15. Experimental results achieved using real cDNA images: (a) observed image, (b) VMF output, (c) ACWVM output.

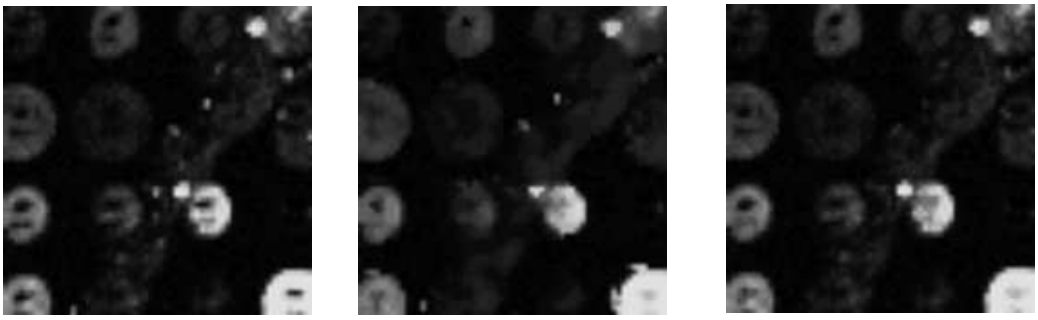

(a) (b) (c)

Fig. 16. Experimental results achieved using real cDNA images: (a) observed image, (b) VMF output, (c) ACWVM output.

Table 3. Results achieved using the test image DNA1.

Noise	5%		10%		15%	
Method	MAE	MSE	MAE	MSE	MAE	MSE
Noisy	3.325	525.2	3.335	528.1	3.338	528.3
VMF	0.135	19.4	0.141	20.3	0.139	20.0
BVDF	0.194	30.4	0.200	31.3	0.198	31.1
DDF	0.135	19.9	0.139	20.5	0.139	20.8
WVMF	0.081	10.4	0.085	11.1	0.082	10.7
CWVMF	0.070	8.9	0.072	9.2	0.070	9.2
ACWVM	**0.069**	**8.0**	0.071	**8.2**	**0.069**	**8.0**

Table 4. Results achieved using the test image DNA2.

Noise	5%		10%		15%	
Method	MAE	MSE	MAE	MSE	MAE	MSE
Noisy	3.231	502.5	3.243	503.8	3.540	550.4
VMF	0.152	21.9	0.161	23.0	0.164	23.7
BVDF	0.224	35.0	0.233	37.1	0.242	38.1
DDF	0.160	23.7	0.164	24.5	0.168	25.2
WVMF	0.085	10.6	0.098	12.4	0.105	13.5
CWVMF	0.071	8.8	0.076	9.6	0.083	10.6
ACWVM	**0.070**	**7.7**	**0.075**	**8.6**	**0.076**	**9.1**

Table 5. Results achieved using the test image DNA3.

Noise	5%		10%		15%	
Method	MAE	MSE	MAE	MSE	MAE	MSE
Noisy	3.673	583.2	3.349	531.9	3.368	536.1
VMF	0.186	29.0	0.174	27.6	0.177	27.9
BVDF	0.267	43.7	0.251	41.4	0.249	40.9
DDF	0.193	31.2	0.177	28.6	0.183	29.7
WVMF	0.100	13.1	0.085	11.3	0.090	12.0
CWVMF	0.088	11.4	0.076	9.8	0.076	9.9
ACWVM	**0.089**	**10.9**	**0.075**	**9.2**	**0.076**	**9.5**

5. Conclusions

In this work a novel algorithm of noise reduction in multichannel images has been presented. Simulation results reveal that this method outperforms the standard procedures used for noise suppression in color images. The new technique has been successfully applied to the denoising of microarray cDNA images. During the filtering process the impulsive noise is being removed while the edges remain well preserved. The proposed technique can serve as an efficient low-processing tool for microarray image enhancement, which can facilitate better spots localization and the estimation of their intensity.

Acknowledgements

The work of the second author was supported by the State Committee for Scientific Research (KBN) in Poland through the grant PBZ 040/P04/08.

References

Ajay N., Tokuyasu T., Snijders A., Segraves R., Albertson D. and Pinkel D. (2002): *Fully automatic quantification of microarray image data*. — Genome Res., Vol. 12, No. 2, pp. 325–332.

Alparone L., Barni M., Bartolini F. and Caldelli R. (1999): *Regularization of optic flow estimates by means of weighted vector median filtering*. — IEEE Trans. Image Process., Vol. 8, No. 10, pp. 1462–1467.

Astola J., Haavisto P. and Neuvo Y. (1990): *Vector median filters*. — Proc. IEEE, Vol. 78, No. 4, pp. 678–689.

Astola J. and Kuosmanen P. (1997): *Fundamentals of Nonlinear Digital Filtering*. — Boca Raton: CRC Press.

Bardos A.J. and Sangwine S.J. (1997): *Selective vector median filtering of colour images*. — Proc. 6th Int. Conf. *Image Processing and Its Applications*, Dublin, Ireland, Vol. 2, pp. 708–711.

Boncelet C. (2000): *Image noise models*, In: Handbook of Image and Video Processing (Bovik A., Ed.). — New York: Academic Press.

Bozinov D. and Rahnenführer J. (2002): *Unsupervised technique for robust target separation and analysis of DNA microarray spots through adaptive pixel clustering*. — Bioinformat., Vol. 18, No. 5, pp. 747–756.

Chen T. and Wu H.R. (2001): *Adaptive impulse detection using center-weighted median filters*. — IEEE Signal Process. Lett., Vol. 8, No. 1, pp. 1–3.

Chen T., Ma K.K. and Chen L.H. (1999): *Tri-state median filter for image denoising*. — IEEE Trans. Image Process., Vol. 8, No. 12, pp. 1834–1838.

Chen Y., Dougherty E.R. and Bittner M.L. (1997): *Ratio-based decisions and the quantitative analysis of cDNA microarray images*. — J. Biomed. Optics, Vol. 2, No. 4, pp. 364–374.

Conway T., Kraus B., Tucker D.L., Smalley D.J., Dorman A.F. and McKibben L. (2002): *DNA array analysis in a Microsoft Windows environment*. — Biotechniques, Vol. 32, No. 1, pp. 110–116.

Dopazo J. (2002): *Microarray data processing and analysis*, In: Microarray Data Analysis II (Lin S.M. and Johnson K.F., Eds.). — Boston: Kluwer, pp. 43–63.

Eisen M.B. and Brown P.O. (1999): *DNA arrays for analysis of gene expression.*. — Methods in Enzymology, Vol. 303, pp. 179–205.

Filkov V., Skiena S. and Zhi J. (2002): *Analysis techniques for microarray time-series data*. — J. Comput. Biol., Vol. 9, No. 2, pp. 317–330.

Gabbouj M. and Cheickh F.A. (1996): *Vector Median-Vector Directional Hybrid Filter for Color Image Restoration*. — Proc. 8th *Europ. Signal Processing Conference, EUSIPCO-96*, Trieste, Italy pp. 879–881.

Hsiao L., Jensen R., Yoshida T., Clark K., Blumenstock J. and Gullans S. (2002): *Correcting for signal saturation errors in the analysis of microarray data*. — Biotechniques, Vol. 32, No. 2, pp. 330–336.

Karakos D.G. and Trahanias P.E. (1997): *Generalized multichannel image-filtering structure*. — IEEE Trans. Image Process., Vol. 6, No. 7, pp. 1038–1045.

Leung Y. (2002): *Microarray data analysis for dummies. . . and experts too?* — Trends Biochem. Sci., Vol. 27, No. 8, pp. 433–434.

Lukac R. (2002): *Color image filtering by vector directional order-statistics*. — Pattern Recognition and Image Analysis, Vol. 12, No. 3, pp. 279–285.

Lukac R. (2003): *Adaptive vector median filtering*. — Pattern Recognition Letters. Vol. 24, No. 12, pp. 1889–1899.

Lukac R. and Marchevsky S. (2001a): *LUM smoother with smooth control for noisy image sequences*. — EURASIP J. Appl. Signal Process., Vol. 2001, No. 2, pp. 110–120.

Lukac R. and Marchevsky S. (2001b): *Adaptive vector LUM smoother*. — Proc. IEEE Int. Conf. *Image Processing, ICIP'2001*, Thessaloniki, Greece, Vol. 1, pp. 878–881.

Lukac R., Smołka B. and Plataniotis K.N. (2002): *Color sigma filter*. — Proc. Int. Workshop *Systems, Signals and Image Processing, IWSSIP'02*, Manchester, U.K., pp. 559–565.

Lukac R., Plataniotis K.N., Smołka B. and Ventesanopulos A.N. (2003a): *Generalized sigmoidal optimization of selection weighted vector filters*. — Proc. IEEE-EURASIP Workshop *Nonlinear Signal and Image Processing, NSIP'03*, Grado, Italy, (accepted).

Lukac R., Plataniotis K.N., Smołka B. and Ventesanopulos A.N. (2003b): *Weighted vector median optimization*. — Proc. 4th EURASIP Conf. *Video/Image Processing and Multimedia Communications, EC-VIP-MC'03*, Zagreb, Croatia, (accepted).

Lucat L., Siohan P. and Barba D. (2002): *Adaptive and global optimization methods for weighted vector median filters*. — Signal Process. Image Comm., Vol. 17, No. 7, pp. 509–524.

Mitra S.J. and Sicuranza G.L. (2001): *Nonlinear Image Processing*. — New York: Academic Press.

Peltonen S., Gabbouj M. and Astola J. (2001): *Nonlinear filter design: Methodologies and challenges*. — Proc. 2nd IEEE Region 8-EURASIP Symp. *Image and Signal Processing and Analysis, ISPA'01*, Pula, Croatia, pp. 102–107.

Pitas I. and Tsakalides P. (1991): *Multivariate ordering in color image filtering*. — IEEE Trans. Circ. Syst. Video Technol., Vol. 1, No. 3, pp. 247–259.

Pitas I. and Venetsanopoulos A.N. (1990): *Nonlinear Digital Filters, Principles and Applications*. — Boston: Kluwer.

Pitas I. and Venetsanopoulos A.N. (1992): *Order statistics in digital image processing*. — Proc. IEEE, Vol. 80, No. 12, pp. 1892–1919.

Plataniotis K.N. and Venetsanopoulos A.N. (2000): *Color Image Processing and Applications*. — Berlin: Springer.

Plataniotis K.N., Androutsos D. and Venetsanopoulos A.N. (1998): *Color image processing using adaptive vector directional filters*. — IEEE Trans. Circ. Syst. II, Vol. 45, pp. 1414–1419.

Schena M., Shalon D., Davis R.W. and Brown P.O. (1995): *Quantitative monitoring of gene expression patterns with a complimentary DNA microarray*. — Science, Vol. 270, pp. 467–470.

Smołka B., Chydziński A., Wojciechowski K., Plataniotis K.N. and Venetsanopoulos A.N. (2001): *On the reduction of impulsive noise in multichannel image processing*. — Optical Eng., Vol. 40, No. 6, pp. 902–908.

Smołka B., Lukac R. and Plataniotis K.N. (2002): *New algorithm for noise attenuation in color images based on the central weighted vector median filter*. — Proc. 9th Int. Workshop *Systems Signals and Image Processing, IWSSIP'02*, Manchester, U.K., pp. 544–548.

Szczepański M., Smołka B., Plataniotis K.N. and Venetsanopoulos A.N. (2002): *Robust Filter for Noise Reduction in Color Images*. — Proc. 1st Europ. Conf. *Color in Graphics, Image and Vision, CGIV'02*, Poitiers, France, pp. 517–522.

Tang K., Astola J. and Neuvo Y. (1995): *Nonlinear multivariate image filtering techniques*. — IEEE Trans. Image Process., Vol. 4, No. 6, pp. 788–798.

Trahanias P.E. and Venetsanopoulos A.N. (1993): *Vector directional filters—a new class of multichannel image processing filters*. — IEEE Trans. Image Process., Vol. 2, No. 4, pp. 528–534.

Trahanias P.E., Karakos D. and Venetsanopoulos A.N. (1996): *Directional processing of color images: Theory and experimental results*. — IEEE Trans. Image Process., Vol. 5, No. 6, pp. 868–881.

Viero T., Oistamo K. and Neuvo Y. (1994): *Three-dimensional median related filters for color image sequence filtering*. — IEEE Trans. Circ. Syst. Video Technol., Vol. 4, No. 2, pp. 129–142.

Yang Y., Buckley M., Dudoit S. and Speed T. (2002): *Comparison of methods for image analysis on cDNA microarray data*. — J. Comput. Graphic Stat., Vol. 11, No. 1, pp. 108–136.

Yin L., Yang R., Gabbouj M. and Neuvo Y. (1996): *Weighted median filters: A tutorial*. — IEEE Trans. Circ. Syst. II, Vol. 43, No. 3, pp. 157–192.